Pure Appl. Chem., Vol. 74, No. 9, pp. 1663–1671, 2002.

Stars and stripes. Nanoscale misfit dislocation patterns on surfaces*

Raghani Pushpa and Shobhana Narasimhan‡

Theoretical Sciences Unit, Jawaharlal Nehru Centre for Advanced Scientific Research, Jakkur P.O., Bangalore 560 064, India

Abstract: Close-packed metal surfaces and heteroepitaxial systems frequently display a structure consisting of regularly spaced misfit dislocations, with a network of domain walls separating face-centered cubic (fcc) and hexagonal close-packed (hcp) domains. These structures can serve as templates for growing regularly spaced arrays of nanoislands. We present a theoretical investigation of the factors controlling the size and shape of the domains, using Pt(111) as a model system. Upon varying the chemical potential, the surface structure changes from being unreconstructed to the honeycomb, wavy triangles, "bright stars", or Moiré patterns observed experimentally on Pt(111) and other systems. For the particular case of Pt(111), isotropically contracted star-like patterns are favored over uniaxially contracted stripes.

INTRODUCTION

Surface science and the study of nanostructures are intimately connected. This is because as the size of an object decreases, its surface-to-volume ratio increases, and surface effects become progressively more important. The atomic arrangement at the surface has important implications for processes taking place at the surface, such as catalysis and growth. In general, surfaces are reconstructed, (i.e., the placement of surface atoms differs from that which would be obtained by a simple truncation of the bulk structure). In the majority of cases, this reconstruction increases the periodicity of the surface structure by a factor of 2 to 10. However, there are cases where the periodicity of the surface structures is significantly increased, to tens of nanometres. In this paper, we will discuss how and why such a situation arises, and its implications and possible applications, focusing on the case of the Pt(111) surface.

The bulk-truncated (111) faces of fcc metals and (0001) faces of hcp metals are close-packed, with every surface atom having a sixfold coordination. This is a fairly low-energy situation, and thus such surfaces are reasonably stable, and were initially thought to be resistant to reconstruction. However, these surfaces are under tensile stress, since surface atoms (having lost their neighbors in layers above) would like to be closer to their neighbors in the surface layer. This preference for an altered interatomic spacing at the surface becomes stronger still for the case of heteroepitaxial systems, where a small number of layers of one metal are deposited on a substrate composed of another metal. Depending on the mismatch between the bulk lattice constants of the substrate and overlayer materials, the stress experienced by atoms in the unreconstructed (for homoepitaxy) or pseudomorphic (for heteroepitaxy) surface can be tensile or compressive (i.e., surface atoms may want to be closer or further apart than the substrate spacing).

Pure Appl. Chem.* **74, 1489–1783 (2002). An issue of reviews and research papers based on lectures presented at the 2nd IUPAC Workshop on Advanced Materials (WAM II), Bangalore, India, 13–16 February 2002, on the theme of nanostructured advanced materials.

‡Corresponding author: E-mail: shobhana@jncasr.ac.in

Reconstruction and misfit dislocation networks

In recent years, scanning tunneling microscopy (STM) and X-ray diffraction experiments have shown that the surface stress in such systems is relieved by the formation of a network of partial misfit dislocations [1]. There are domains where surface atoms continue the bulk stacking sequence and sit in either the fcc sites [for fcc(111) surfaces] or hcp sites [for hcp(0001) surfaces]. However, these alternate with domains where surface atoms sit in faulted sites, either hcp [for fcc(111) surfaces] or fcc [for hcp(0001) surfaces]. Although it costs some energy to make these stacking faults, there is a trade-off, as this alternation between fcc and hcp stacking provides a low-energy route to altering the surface density.

Homoepitaxy: Au(111)

The first metallic system in which these phenomena were observed is the Au(111) surface, which shows a "herringbone" pattern comprised of "double stripes" whose orientation changes periodically, alternating between two out of three equivalent directions along the surface [2,3]. Each double stripe consists of a wide fcc domain and a narrower hcp domain, separated by domain walls where atoms sit near the bridge sites (halfway between the fcc and hcp sites). Atoms at bridge sites are pushed out of the surface plane, and thus show up as light regions on STM images. The periodicity of the double stripe is $22a$, where a is the bulk nearest-neighbor distance. The double stripe contains two partial misfit dislocations, with the net effect that 23 surface atoms sit in the distance of $22a$, (i.e., the surface density has been increased uniaxially). To form the herringbone out of the double stripe, the stripes bend at "elbows". Alternate domain walls contain either rounded or pointed elbows; there are point dislocations at pointed elbows. Figure 1 shows a simulated STM image of the herringbone pattern [3].

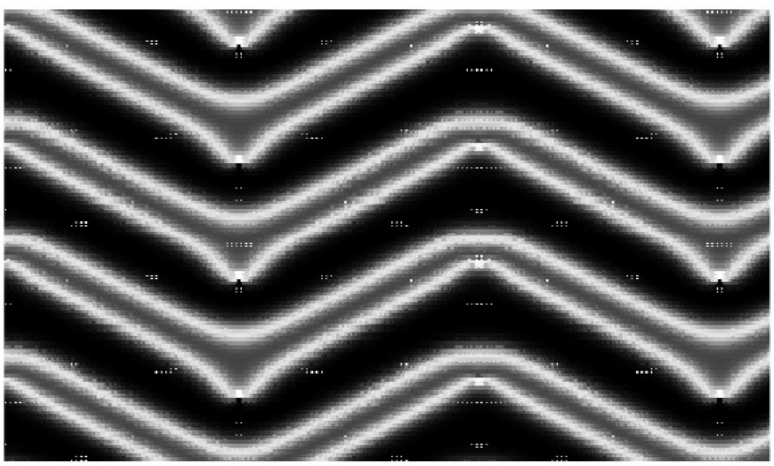

Fig. 1 A simulated STM image showing the herringbone pattern on Au(111) [3].

Homoepitaxy: Pt(111)

Subsequently, somewhat similar misfit dislocation patterns were observed on Pt(111). Unlike Au(111), Pt(111) does not reconstruct under normal conditions of temperature and pressure. However, experiments have shown that it can be induced to reconstruct, either by raising the temperature above 1330 K [4], or by placing the surface in a supersaturated Pt vapor [5]. In both cases, the surface was found to reconstruct into a pattern that is similar to that of Au(111), in that it is built up out of a basic motif of the double stripe; however, instead of the domain walls (misfit dislocations) forming a herringbone pat-

tern, they form a honeycomb network. In addition, on certain dense terraces of Pt(111), the honeycomb reconstruction was found to be modified into a pattern of wavy triangles [6].

Heteroepitaxial systems

Similar structures, formed by hcp and fcc domains separated by networks of partial misfit dislocations, are found also in several heteroepitaxial systems. The shape and size of the domains, however, do vary considerably from system to system. For example, the second layer of Ag on Pt(111) [7], and the second layer of Cu on Ru(0001) [8] show a double stripe pattern (without any herringbone superstructure); on annealing, the former is transformed to a trigonal network of misfit dislocations [7]. In contrast, Na on Au(111) [9] and 3 ML of Cu on Ru(0001) [8] show triangular domains forming a "bright star pattern", which is somewhat similar to that seen when Ni is deposited on Ru(0001) [10], although the domain walls are straighter in the latter case. Four ML of Cu on Ru(0001) results in a hexagonal Moiré pattern, where all sites on the surface are occupied, including the top sites (where surface atoms sit directly above atoms in the layer below) [8].

TEMPLATES FOR GROWING NANOSTRUCTURES

Recently, a great deal of interest has been focused on such reconstructions and misfit dislocation networks, primarily because it has been shown that they can be used as templates for growing ordered nanostructures. For example, if Ni [11], Co [12], or many other metals are deposited on Au(111), nearly monodisperse islands of the overlayer nucleate at the pointed elbows of the underlying herringbone reconstruction. Because of the regular periodicity of the herringbone, these islands form a regularly spaced two-dimensional array with nanometre spacing. Subsequently, similar effects have been observed in several other heteroepitaxial systems. For example, the deposition of Fe on a Cu bilayer on Pt(111), and the deposition of Ag on an Ag bilayer on Pt(111) result in a regular hexagonal array of nanoislands [13].

One can envisage a wide range of possible applications for such nanostructures, e.g., if the nanoislands are composed of a magnetic material, one could hope to use such structures for information storage; alternatively, if they are composed of a catalytically active material, one could make nanoscale chemical reactors. For most of these applications, one would like to have control over the spacing and geometry of these arrays of islands, which in turn implies understanding and controlling the underlying reconstruction/misfit dislocation pattern. The work that we will describe below is, in part, motivated by these considerations.

We will focus on Pt(111), partly because it serves as a useful model system for some of the issues that we are interested in. In addition, of course, any information about the structure of Pt(111) is of great interest, because of the importance of this surface as a catalyst in a number of commercially and scientifically important chemical reactions.

CALCULATIONS

We have used a generalized version of the Frenkel–Kontorova model, parametrized by ab initio calculations, to study the surface structure. In general, the formation of surface structures like the ones we are interested in involves a fairly delicate balance between various contributions to the total energy, and, therefore, it is desirable to describe the interatomic interactions as accurately as possible. Currently, this can best be done by performing ab initio calculations within the framework of density functional theory. However, the computational cost of such calculations increases enormously as the size of the unit cell becomes larger. For the kinds of large-period patterns seen on these surfaces, there are typically several thousand atoms per layer in the unit cell, and, therefore, it becomes prohibitively expensive to per-

form ab initio calculations on these surfaces. Therefore, we do the next best thing: we use ab initio calculations to parametrize a model; an approach that is found to be very successful.

Frenkel–Kontorova model

The application of the Frenkel–Kontorova (FK) model [14] to the study of misfit dislocations has a long history [15]. This model captures the essential physics that determines whether or not such stacking faults and dislocations are formed. The Hamiltonian is given by:

$$H = \sum_i V_{ss}(l_i) + \sum_j V_{sb}(\boldsymbol{r}_j) + \Gamma N, \quad (1)$$

where the first summation runs over all nearest-neighbor (NN) bonds between surface atoms, and the second runs over all atoms in the surface layer. The interaction between two surface atoms, V_{ss}, depends on the bond length l_i, and has its minimum at a distance b, which differs from a, the NN distance in the bulk, (i.e., surface atoms would like to be at a separation $b \neq a$). However, this tendency toward densification/expansion is opposed by the substrate potential V_{sb}, which has its global minimum when the atom positions $\boldsymbol{r}_j$ fall at fcc sites (i.e., this term will penalize any deviation from the bulk stacking sequence). The importance of adding the third term, ΓN to the Hamiltonian in eq. 1 (where N is the number of atoms in the surface layer) has been pointed out by Mansfield and Needs [16]. These are reconstructions in which the density of surface atoms differs for the reconstructed and unreconstructed surface, and Γ is in the nature of a chemical potential, specifying the energy cost of obtaining extra atoms for incorporation into the surface layer. The value of Γ depends upon where these additional atoms are obtained from.

To summarize: the first term in eq. 1 favors reconstruction, the second opposes it, and the third term will either oppose it (when Γ is positive) or favor it (when Γ is negative). Whether or not the surface reconstructs, is determined by which combination of terms wins out. One can determine the atomic positions by minimizing the surface energy (total energy per unit area), using the Hamiltonian of eq. 1.

One-dimensional versions of the FK model, where V_{sb} is either a sine or double-sine potential, were initially used to study the reconstruction of Au(111) [17] and to determine the stability of fcc(111) surfaces [16]. Subsequently, two-dimensional generalizations of the model have been used to study the reconstruction of Au(111) [18,3], Cu/Ru(0001) [19], and Ag/Pt(111) [20]; using parameters variously derived from ab initio calculations or merely an appeal to physical reasonableness. We use a similar approach, except that our parameters are obtained *entirely* from ab initio calculations.

Ab initio calculations on Pt

The ab initio calculations were performed using the PWSCF package [21], using a plane-wave basis, and ultrasoft pseudopotentials with a cut-off of 20 Ry; a higher cut-off of 160 Ry was used to expand the augmentation charges associated with the use of the ultrasoft pseudopotential. Bulk calculations were done using both the fcc primitive unit cell, and a $1 \times 1 \times 15$ supercell containing a repeating slab of 15 bulk layers stacked along [111]; surface calculations were performed using the same supercell, containing 9 layers of atoms stacked along [111], and a vacuum of thickness equivalent to 6 layers. It was verified that these thicknesses of the slab and vacuum were sufficient to obtain converged results for the quantities of interest to us. Brillouin zone integrations were carried out using 110 points within the irreducible Brillouin zone (IBZ) of the fcc cell, and 27 points within the IBZ of the slab cells. For the bulk, total energies obtained using the two cells were practically identical, indicating that good convergence has been achieved. For the calculations on the flat surface, the three layers in the middle of the slab were fixed, and the top three and bottom three layers were allowed to move. To determine the adatom adsorption energy, we used a $3 \times 3 \times 12$ supercell, containing 5 layers stacked along [111], each containing 9 Pt atoms, a single adatom adsorbed on an fcc site, and 6 vacuum layers. The coordinates of the adatom and all atoms in the top two surface layers were allowed to vary.

We obtained the bulk lattice constant $a_0 = \sqrt{2}a$ as 3.92 Å, the cohesive energy E_b as 0.54 Ry, the surface energy γ as 9.13 mRy/Å^2, and the surface stress σ as 29.45 mRy/Å^2. For the adatom absorption energy E_a, we obtain a value of 0.43 Ry. These results are in good agreement with experiments and the results of previous calculations of these quantities [22,23,16].

In order to determine the potential between surface atoms, we compressed the slab of Pt atoms in the *xy*-plane (the *z* axis is oriented along [111]) and calculated the variation in the surface stress as a function of the in-plane lattice constant l_{xy}. These results are shown in Fig. 2.

Finally, in order to obtain the substrate potential V_{sb}, we computed the energy it costs to make surface stacking faults, when surface atoms occupy hcp, bridge and top sites instead of the most favored fcc site. The energy cost per surface atom was found to be 5.05, 5.89, and 11.85 mRy, respectively.

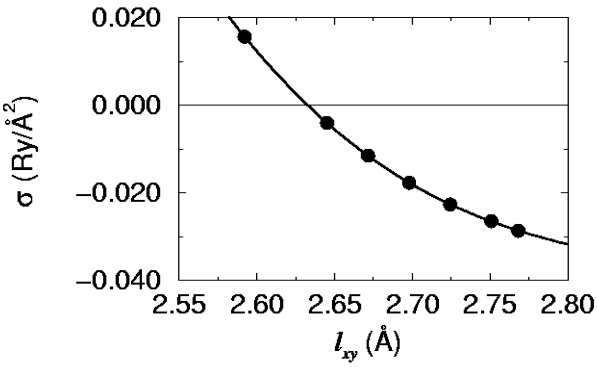

Fig. 2 Results from ab initio calculations for the variation of the surface stress as a function of the in-plane lattice constant l_{xy}, for Pt(111). This result is used to obtain the interaction between surface atoms.

Parametrizing the Frenkel–Kontorova model

Upon fitting to the results for surface stress shown in Fig. 2, we find that the surface–surface interactions can be well described by a Morse form: $V_{ss}(r) = A_0\{1 - \exp[-A_1(r - b)]\}^2$. The best fit is obtained with the values: A_0 = 60.2 mRy, A_1 = 2.062 Å^{-1}, and b = 2.638 Å.

For the surface–bulk interaction, we obtain the substrate potential $V_{sb}(x,y)$ for an atom at an arbitrary position (x,y) in the surface plane by expanding our results at fcc, hcp, bridge and top sites, using a 2-dimensional Fourier expansion involving the first two shells of reciprocal lattice vectors; this is standard practice [3,18–20].

For the chemical potential Γ, we are interested in two cases: when the extra atoms come from the bulk (or step edges, since the binding energy of an atom at a step edge is almost equal to that of a bulk atom), and when they come from adatoms. The latter case becomes especially relevant for the situation when the surface is placed in a supersaturated vapor, since there is then the deposition of a large number of adatoms upon the flat surface. These adatoms can, presumably, be more easily incorporated into the surface layer. For the bulk case, we find Γ_b= 50.56 mRy, whereas for adatoms, Γ becomes negative, with Γ_a = –67.12 mRy. In general, $\Gamma_a \leq \Gamma_b$.

Results from energy minimization

We determine whether or not the surface reconstructs, and the optimal positions of surface atoms, by minimizing the Hamiltonian of eq. 1, per unit area. We are searching for the optimal value of $\Delta\rho$, the increase in density in the surface layer. We consider two cases: (i) "stripes", involving uniaxial compression along the [1 $\bar{1}$ 0] direction; (ii) "stars", involving isotropic compression in the surface plane.

For the latter case, there is another parameter that we have to optimize: θ, the angle between the unit vectors of the surface layer and the substrate.

Figure 3 shows our results, for both uniaxial and isotropic compression, for the two extreme values of chemical potential, Γ_a and Γ_b. We have plotted $\Delta\gamma$, the difference in the surface energies of the reconstructed (compressed) and unreconstructed (uncompressed) structures, as a function of the increase in density $\Delta\rho$. It can be seen that: (i) for both the "stripe" and the "star", the surface will not reconstruct under normal conditions, but will reconstruct when the chemical potential is lowered further. In both cases, the surface reconstructs (and a misfit dislocation network is formed) when all the additional density is obtained from adatoms. (ii) The "stars" (isotropic compression) are always favored over the "stripes" (uniaxial compression). (An earlier simulation of the Pt(111) surface also studied the stripe, and found that it can lower the energy, relative to the unreconstructed surface; however, the authors of this paper did not study the energetics of the repeating pattern of "stars" [25].) It should be emphasized that this result holds only for the particular case of Pt(111), and explains why experiments do not observe the double stripe pattern on Pt(111) surfaces.

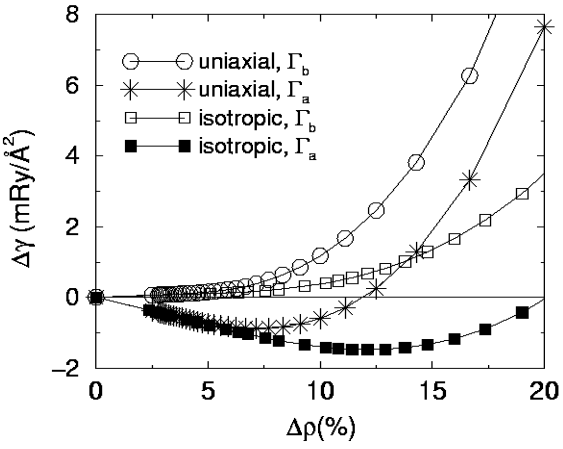

Fig. 3 Results showing how $\Delta\gamma$, the difference in the surface energy of the reconstructed and unreconstructed surfaces, varies with $\Delta\rho$, the increase in the density of the top layer. We show the results for both the uniaxial (stripe) and isotropic (star) cases, for the two extreme cases of chemical potential, Γ_a and Γ_b.

Domain patterns and misfit dislocation networks

For applications in nanotechnology, we obviously want to know not just whether such misfit dislocation networks are formed, but the size and shape of domains, as this will serve as the template for the nucleation of islands.

In order to visualize the surface structure, we use a simple technique to obtain the surface topography and thus simulate an STM image. We obtain the height of a surface atom at an arbitrary position (x,y) using a technique similar to that used to obtain the substrate potential $V_{sb}(x,y)$, as described above. We will use a 2-dimensional Fourier expansion about the heights at fcc, hcp, bridge and top sites. From our ab initio computations of stacking fault systems, we find these heights to be 0, 0.03, 0.07, and 0.29 Å, respectively. Of course, these values have been obtained for the case where the entire top layer occupies faulted sites, whereas the structures we are interested in display a distribution of faulted stacking. However, these numbers serve as rough guidelines, and, above all, suffice to bring out the geometry of the reconstructed structure. We will shade each atom according to its height, with black corresponding to the lowest atoms (at fcc sites), and white corresponding to the highest atoms (at top sites).

In Figs. 4 and 5, we show a series of such simulated STM patterns. Figure 4 shows the uniaxial stripe pattern, for $\Delta\rho$ = 2 %. The repeating double stripe is clearly seen; it has a periodicity of $50a$ = 138.4 Å. For this pattern, no atoms occupy the top sites, and therefore there are no white regions in this image. The wider and narrower darker regions correspond to regions where atoms occupy fcc and hcp sites respectively; note how narrow the hcp region is. The lighter stripes correspond to the domain walls separating the fcc and hcp domains; atoms here sit close to the bridge sites halfway between fcc and hcp sites. In Fig. 5, we show how the "star" patterns change as the density in the top

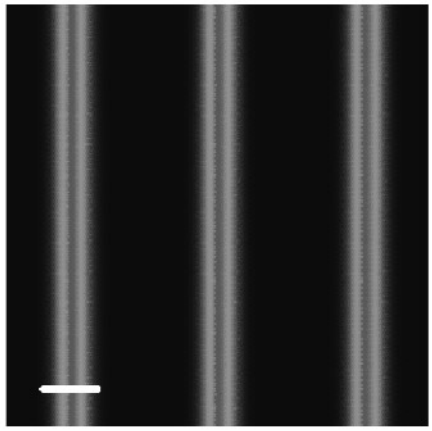

Fig. 4 Simulated STM image of the uniaxial stripe reconstruction on Pt(111), for an increase in density of 2 %. The white line marked on the figure indicates a length of 50 Å.

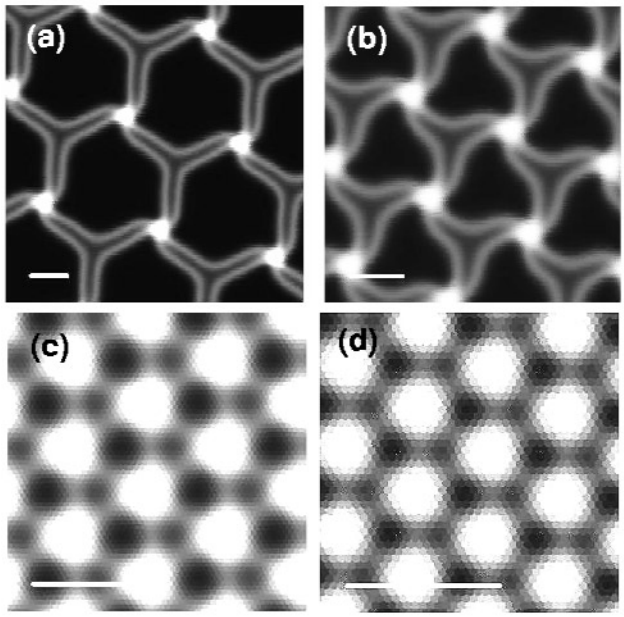

Fig. 5 Simulated STM images showing the isotropic "star" patterns. The size and shape of the domains evolves as the density in the top layer is increased, relative to the unreconstructed surface, by (a) 3.1 %, (b) 5.1 %, (c) 11.4%, and (c) 17.4 %. The four figures show, respectively, the honeycomb, the wavy triangles, the bright stars, and the Moiré pattern.

layer is increased. Figure 5a shows the honeycomb pattern; its kinship to the double stripe of Fig. 4 is evident, with the double stripes now being arranged along three directions to form the honeycomb network. The large dark hexagons are the fcc domains, and the narrow dark strips are the hcp domains; once again these are separated by the lighter domain walls. As the density in the top layer is increased, it can be seen that the honeycomb is transformed into first a pattern of wavy triangles, then the straight-rayed "bright star", and then the Moiré pattern. As the density of the top layer is increased, the periodicity of the pattern decreases. One notable feature in the honeycomb and wavy triangles are the "bright rotors"—the rays (domain walls) that emerge from the bright centers (regions where atoms sit at top sites) have a whorl-like appearance. This results from the rotation of the top layer relative to the substrate, which breaks the reflection symmetry otherwise present on the surface.

CONCLUSIONS

For the particular case of Pt(111), we have confirmed that the surface does not reconstruct under normal circumstances, but can be induced to reconstruct by the adsorption of a large number of adatoms. In fact, a stability analysis shows that the unreconstructed Pt(111) surface is very close to being unstable [26]. This explains why a relatively small change in the chemical potential can induce the surface to reconstruct. We also believe that this explains the temperature-induced reconstruction of this surface: owing to the thermal expansion of interlayer spacings, at higher temperatures, V_{sb} becomes considerably flatter, thus favoring a reconstruction even at the bulk chemical potential. Given the importance of Pt(111) as a catalyst, its tendency towards structural instability is certainly noteworthy.

From our simulated STM images, it is clear that there is an evolution of shape and size in the misfit dislocation patterns formed when the surface reconstructs. It is this aspect of our work that is most relevant to applications in nanotechnology. All the star-like patterns are characterized by bright centers where atoms sit at top sites. From these bright centers, six rays or domain walls emerge. It is the arrangement of these domain walls that determines the pattern, and, accordingly, we obtain most of the domain geometries observed hitherto in homoepitaxial and heteroepitaxial systems. The fact that there is a smooth transition between the various patterns (something that is evident from an examination of the images in Fig. 5) shows that the same physical factors are operating in all these different systems, and it is only slight differences in parameters (and hence the favored density) that are responsible for the different patterns seen. By a suitable choice of system, chemical potential, and temperature, one should be able to achieve any desired periodicity.

REFERENCES

1. For reviews, see H. Brune. *Surf. Sci. Rep.* **31**, 121 (1998); F. Besenbacher. *Rep. Prog. Phys.* **59**, 1737 (1996).
2. J. V. Barth, H. Brune, G. Ertl, R. J. Behm. *Phys. Rev. B* **42**, 9307 (1990).
3. S. Narasimhan and D. Vanderbilt. *Phys. Rev. Lett.* **69**, 1564 (1992).
4. A. R. Sandy, S. G. J. Mochrie, D. M. Zehner, G. Grübel, K. G. Huang, D. Gibbs. *Phys. Rev. Lett.* **68**, 2192 (1993).
5. M. Bott, M. Hohage, T. Michely, G. Comsa. *Phys. Rev. Lett.* **70**, 1489 (1993).
6. M. Hohage, T. Michely, G. Comsa. *Surf. Sci.* **337**, 249 (1995).
7. H. Brune, H. Röder, C. Boragno, K. Kern. *Phys. Rev. B* **49**, 2997 (1994).
8. C. Günther, J. Vrijmoeth, R. Q. Hwang, R. J. Behm. *Phys. Rev. Lett.* **74**, 754 (1995).
9. J. V. Barth, R. J. Behm, G. Ertl. *Surf. Sci. Lett.* **302**, L319 (1994).
10. J. A. Meyer, P. Schmid, R. J. Behm. *Phys. Rev. Lett.* **74**, 3864 (1995).
11. D. D. Chambliss, R. J. Wilson, S. Chiang. *Phys. Rev. Lett.* **66**, 1721 (1991).
12. B. Voigtländer, G. Meyer, N. M. Amer. *Phys. Rev. B* **44**, 10354 (1991).
13. H. Brune, M. Giovannini, K. Bromann, K. Kern. *Nature* **394**, 451 (1998).

14. J. Frenkel and T. Kontorova. *Z. Sowjetunion* **13**, 1 (1938).
15. F. C. Frank and J. H. van der Merwe. *Proc. R. Soc.* **198**, 205 (1948).
16. M. Mansfield and R. J. Needs. *J. Phys. Condens. Matter* **2**, 2361 (1990).
17. M. El-Batanouny, S. Burdick, K. M. Martini, P. Stancioff. *Phys. Rev. Lett*. **58**, 2762 (1987); R. Ravelo and P. El-Batanouny. *Phys. Rev. B* **40**, 9574 (1989).
18. N. Takeuchi, C. T. Chan, K. M. Ho. *Phys. Rev. B* **43**, 13899 (1991).
19. J. C. Hamilton and S. M. Foiles. *Phys. Rev. Lett.* **75**, 882 (1995).
20. J. C. Hamilton, R. Stumpf, K. Bromann, M. Giovannini, K. Kern, H. Brune. *Phys. Rev. Lett.* **82**, 4488 (1999).
21. S. Baroni, A. Dal Corso, S. de Gironcoli, P. Giannozzi. http://www.pwscf.org
22. R. J. Needs and M. Mansfield. *J. Phys. Condens. Matter* **1**, 7555 (1989).
23. P. J. Feibelman, J. S. Nelson, G. L. Kellogg. *Phys. Rev. B* **49**, 10548 (1994); P. J. Feibelman. *Phys. Rev. B* **56**, 2175 (1997).
24. G. Boisvert, L. J. Lewis, M. Scheffler. *Phys. Rev. B* **57**, 1881 (1998).
25. J. Jacobsen, K. W. Jacobsen, P. Stolze. *Surf. Sci.* **317**, 8 (1995).
26. S. Narasimhan and R. Pushpa. Submitted for publication.